23rd ABCM International Congress of Mechanical Engineering
December 6-11, 2015, Rio de Janeiro, RJ, Brazil

NUMERICAL ANALYSIS OF THE INFLUENCE OF THREE TURBULENCE MODELS ON THE PREDICTION OF THE AIRFLOW INSIDE A LOW SPEED WIND TUNNEL

Guilherme Loyola França de Vasconcellos
Caio Dell'Oro de Oliveira
Antônio Augusto Mesquita Diniz
Sérgio de Morais Hanriot
Cristiana Brasil Maia
Departament of Mechanical Engineering, Pontíficia Universidade Católica de Minas Gerais – Puc Minas, Av. Dom José Gaspar, 500, Coração Eucarístico, Belo Horizonte MG, Brazil, 30535-901
guivasconcellos@hotmail.com, cacadelloro@hotmail.com, antonioaugustodiniz@hotmail.com hanriot@pucminas.br, cristiana@pucminas.br

Abstract. *Two important tools are used to perform aerodynamic studies: experimental tests, usually conducted in wind tunnels; and numerical tests, using Computational Dynamic Fluids (CFD) techniques. In this paper, it was performed a numerical analysis of the behavior of the airflow in a low-speed wind tunnel, using the commercial software Ansys CFX®. This study aimed to evaluate the ability of the turbulence model to predict the airflow parameters inside a low-speed wind tunnel. Three turbulence models, based on Reynolds-Averaged Navier-Stokes (RANS), κ-ε, k-ω SST and BSL EARSM, were used. The dimensions of the wind tunnel represent a device located at Pontifícia Universidade Católica of Minas Gerais, Brazil. The results were compared to experimental data obtained in the experimental device. Numerical results showed that the k- ω SST and BSL EARSM models return closer results to experimental data, which can be explained by the low performance of the κ-ε model on the prediction of internal flows in regions near the walls.*

Keywords: *Wind Tunnel, CFD, Turbulence model, k- ω SST, BSL EARSM, κ-ε model, RANS.*

1. INTRODUCTION

Wind Tunnel (WT herein after) tests have been performed since a long time and their development was driven by the advent of aviation industry around 1900 (Baker, 2007). Wright brother's built up their glider number three with aid of a WT (Green; Quest 2011). Today, low speed WT's tests are becoming powerful and important tools for studies and research related to aerodynamic phenomena. Measurements are performed in order to evaluate the effect of the velocity on the drag and lift forces, for instance, as studied by Cho and Kim (2011). These devices are used in problems associated with fluid dynamics, in the fluid-structure interaction, specially related to aeronautics and automobile industries, environment (effects of smoke dispersion in environments encountered in daily life) and construction. Calautit and Hughes (2014) studied the effects of the air flow in a commercial tower under the effect of several wind directions. For accomplishing this objective, an experimental approach technique was used through a WT and numerical CFD techniques by using standard κ-ε turbulence model. The data obtained from wind tunnel tests are most part of the time used for validate Computational Fluid Dynamics (CFD) calculations.

Although today experimental data are a reliable tool widely used by the industry, its reliability from tests in wind tunnel depends on knowledge of the flow quality in the test section (Reis; Falcão Filho; Morais, 2014). It is quite important to have a controlled and characterized flow in a wind tunnel to ensure repeatability and to allow comparison between theory and modeling (Merrinson *et al*, 2008). Thus, the knowledge of the flow inside a WT is a serious work.

CFD techniques can be used to develop models for the aerodynamic problems, to evaluate the influence of several parameters on the analysis, and to help experimental results by comparing experimental and numerical data (Abdi, 2014). Nowadays, it has reached a stage in which its direct combination with the wind tunnel approach can yield a synergistic effect, being used as a tool to support wind tunnel design, testing and interpretation of results (Moonen et al, 2006). For a good CFD analysis of the flow behavior, it is always important to conduct simulations with the highest number of turbulence models, as done by Tong *et al* (2012).

Several researches have been developed using CFD to evaluate problems associated with aerodynamics. Defraeye (2010) studied the flow around a cyclist in different position. The simulation was made using different turbulence methodologies, like RANS and LES. Calautit, Hughes and Shahzad (2015) used CFD modelling and scaled wind tunnel testing to evaluate the performance of a standard and a heat transfer device wind catcher. CFD simulations were generally in good agreement with the measurements.

This paper evaluates the effect of three turbulence models on the prediction of the airflow inside a low speed wind tunnel. Numerical results are compared to experimental data.

2. MATHEMATICAL MODEL

The presented problem can be described through the mass (Eq. 1) and momentum (Eqs. 2-4) conservation equations:

$$\frac{\partial \rho}{\partial t} + \vec{\nabla}.(\rho \vec{V}) = 0; \tag{1}$$

ρ is the specific fluid mass and $\vec{V}$ the velocity vector.

$$\rho\left(\frac{\partial \bar{u}}{\partial t} + u\frac{\partial \overline{uu}}{\partial x} + v\frac{\partial \overline{uv}}{\partial y} + w\frac{\partial \overline{uw}}{\partial z}\right) = -\frac{\partial P'}{\partial x} + \mu\frac{\partial^2 u}{\partial x^2} - \left[\frac{\partial\left(\rho\overline{u'^2}\right)}{\partial x} + \frac{\partial\left(\rho\overline{u'v'}\right)}{\partial y} + \frac{\partial\left(\rho\overline{u'w'}\right)}{\partial z}\right] + S_{Mx} \tag{3}$$

$$\rho\left(\frac{\partial \bar{v}}{\partial t} + u\frac{\partial \overline{vu}}{\partial x} + v\frac{\partial \overline{vv}}{\partial y} + w\frac{\partial \overline{vw}}{\partial z}\right) = -\frac{\partial P'}{\partial y} + \mu\frac{\partial^2 v}{\partial y^2} - \left[\frac{\partial\left(\rho\overline{u'v'}\right)}{\partial x} + \frac{\partial\left(\rho\overline{v'^2}\right)}{\partial y} + \frac{\partial\left(\rho\overline{v'w'}\right)}{\partial z}\right] + S_{My} \tag{4}$$

$$\rho\left(\frac{\partial \bar{w}}{\partial t} + u\frac{\partial \overline{wu}}{\partial x} + v\frac{\partial \overline{wv}}{\partial y} + w\frac{\partial \overline{ww}}{\partial z}\right) = -\frac{\partial P'}{\partial z} + \mu\frac{\partial^2 w}{\partial z^2} - \left[\frac{\partial\left(\rho\overline{u'w'}\right)}{\partial x} + \frac{\partial\left(\rho\overline{w'v'}\right)}{\partial y} + \frac{\partial\left(\rho\overline{w'^2}\right)}{\partial z}\right] + S_{Mz} \tag{5}$$

The momentum conservation equations are presented for turbulent flows, as show in Warsi (2006). u, v and w are the velocity components in each direction x, y and z respectively, u ', v' and w' the fluctuations of the velocity components, μ is the dynamic viscosity of the fluid, S_{Mx}, S_{My} and S_{Mz} are the source terms and P 'is the static pressure fluctuation. The Reynolds's are modeled as (Versteeg; Malalasekera, 2007):

$$\tau_{ij} = \rho\,\overline{u_i'u_j'} = \mu_t\left(\frac{\partial U_i}{\partial x_j} + \frac{\partial U_j}{\partial i}\right) - \frac{2}{3}\rho\kappa\delta_{ij} \tag{6}$$

κ is the turbulent kinetic energy of the flow per unit mass and δij represents the Kronecker's delta. In the κ-ε model, the turbulent viscosity μ_t is written as (Warsi, 2006),

$$\mu_t = \rho C_\mu \frac{\kappa^2}{\varepsilon} \tag{7}$$

Cμ is a dimensionless constant and ε the dissipation rate of turbulent kinetic energy. The transport equations for the turbulent kinetic energy and for the dissipation rate of energy ε are (Veersteg, Malalasekera, 2007):

$$\frac{\partial(\rho\kappa)}{\partial t} + \nabla\cdot\left(\rho\kappa\vec{U}\right) = \nabla\cdot\left[\left(\frac{\mu_t}{\sigma_\kappa}\right)\nabla(\kappa)\right] + 2\mu_t S_{ij}.S_{ij} - \rho\varepsilon \tag{8}$$

$$\frac{\partial(\rho\varepsilon)}{\partial t} + \nabla\cdot\left(\rho\varepsilon\vec{U}\right) = \nabla\cdot\left[\left(\frac{\mu_t}{\sigma_\varepsilon}\right)\nabla(\varepsilon)\right] + C_{1\varepsilon}\frac{\varepsilon}{\kappa}2\mu_t S_{ij}.S_{ij} - C_{2\varepsilon}\rho\frac{\varepsilon^2}{\kappa} \tag{9}$$

The constants represented in κ-ε model are: Cμ=0,09, σκ=1,00, σε=1,30, C1ε=1,44 e C2ε=1,92.

The κ-ω SST turbulence model, proposed by Menter (1992), applies a mix of features which uses κ-ω of Wilcox in regions close to the wall and κ-ε to free flow regions. In this model the calculation of the Reynolds's stresses and turbulent kinetic energy of the system are the same as those used by κ-ε standard model, but the dissipation rate of the turbulent kinetic energy is transformed into dissipation frequency, ω given in Eq (10)

$$\varepsilon = \kappa\omega \tag{10}$$

Thus both differential equation added by SST are those of the turbulent kinetic energy, Eq. (11), and the dissipation frequency of the turbulent kinetic energy, ω, Eq. (12).

$$\frac{\partial(\rho\kappa)}{\partial t} + \nabla\cdot\left(\rho\kappa\vec{V}\right) = \nabla\cdot\left[\left(\mu + \frac{\mu_t}{\sigma_\kappa}\right)\nabla(\kappa)\right] + P_\kappa - \beta^*\rho\kappa\omega \tag{11}$$

$$\frac{\partial(\rho\omega)}{\partial t} + \nabla\left(\rho\omega\vec{V}\right) = \nabla\left[\left(\mu + \frac{\mu_t}{\sigma_{\omega,t}}\right)\nabla(\omega)\right] + \gamma_2\left(2\rho S_{ij}.S_{ij} - \frac{2}{3}\rho\omega\frac{\partial V_i}{\partial x_j}\delta_{ij}\right) - \beta_2\rho\omega^2 + 2\frac{\rho}{\sigma_{\omega,2}\omega}\frac{\partial\kappa}{\partial x_\kappa}\frac{\partial\omega}{\partial x_\kappa} \tag{12}$$

The constants represented in SST model are: σκ=1,0; σw,1 = 2,0; σw,2 = 1,17; γ2=0,44; β2= 0,083 e β*= 0,09.

The turbulence model BSL RSM (Reynolds Stress Model) introduces seven new equations to solve the closure problem. Of the seven new equations one is to transport the turbulent kinetic energy and the other six to solve each one of the independent Reynolds's stresses. However, due to the high number of additional equations, it was proposed the BSL EARSM (Baseline Explicit Algebraic Reynolds Stress Model), where the terms of diffusion and convection from the RSM model are reduced to algebraic equations. The mathematical formulation, as exposed by Chung (2002), is:

$$\frac{D\kappa}{Dt} = \nabla\cdot\left(\left(\nu + \sigma_\kappa\nu_t\right)\nabla\kappa\right) + \tilde{P}_\kappa - \beta^*\kappa\omega \tag{13}$$

$$\frac{D\omega}{Dt} = \nabla\cdot\left(\left(\nu + \sigma_\omega\nu_t\right)\nabla\omega\right) + \frac{\gamma\omega}{\kappa}\tilde{P}_\kappa - \beta\omega^2 + \frac{\sigma_d}{\omega}(\nabla\kappa)\cdot(\nabla\omega) \tag{14}$$

$\tilde{P}_k$ is given by:

$$\tilde{P}_\kappa = \min\left(-\tau_{ij}\frac{\partial U_i}{\partial x_j}, 10\cdot\rho\beta^*\kappa\omega\right) \tag{15}$$

The EARSM's constants depend on the F1 blended function, presented in Table 1 and Eq. (16)

Table 1 - Constants of BSL EARSM model

BSL EARSM Model		
$\sigma_\kappa = F_1\sigma_{\kappa1} + (1-F_1)\sigma_{\kappa2}$	$\sigma_{k1} = 0.5$	$\beta_1 = 0.075$
$\sigma_\omega = F_1\sigma_{\omega1} + (1-F_1)\sigma_{\omega2}$	$\sigma_{k2} = 0.5$	$\beta_2 = 0.083$
$\beta = F_1\beta_1 + (1-F_1)\beta_2$	$\sigma_{\omega1} = 0.5$	$\beta^* = 0.09$
$\sigma_d = 2(1-F_1)\sigma_{\omega2}$	$\sigma_{\omega2} = 0.856$	$\gamma = \frac{\beta}{\beta^*} - \frac{\sigma_\omega\kappa^2}{\sqrt{\beta^*}}$

$$F_1 = \tanh\left(\left\{\min\left[\max\left(\frac{\sqrt{\kappa}}{C_\mu\omega d}, \frac{500\nu}{\omega d^2}\right), \frac{2\kappa\omega}{d^2(\nabla\kappa)\cdot(\nabla\omega)}\right]\right\}^4\right) \tag{16}$$

3. NUMERICAL METHODOLOGY

The geometry of the wind tunnel used in the numerical simulation was based on a low speed wind tunnel of Pontifícia Universidade Católica de Minas Gerais, situated in the city of Belo Horizonte. The prototype has a blower, a stagnation section, a contraction section and a squared test section, with a edge size of 200 mm. The wind tunnel operates with an open circuit and has 3140 mm of length. The test section has 940 mm, the contraction section has 795 mm and the stagnation section has 1095 mm (Fig. 1).

The numerical analysis was performed using the CFX® Ansys 14.5 software. The most important assumptions for solving the numerical problem in question were:

- Air as ideal gas;
- Steady state conditions;
- Isothermal flow at 15ºC;
- Static Pressure of 1 atm (101.325 kPa)

The boundary conditions used are:

- Relative static pressure at the exit of 0 Pa.
- No-slip conditions close to the wall;
- Impermeable wall;
- Imposed mass flow of 0.303 kg/s at the inlet;
- Turbulent intensity of 5%.

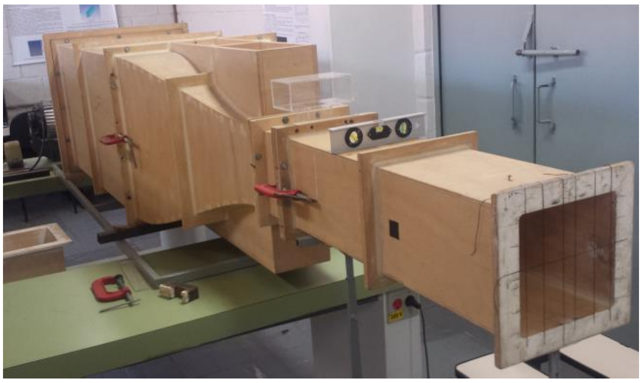

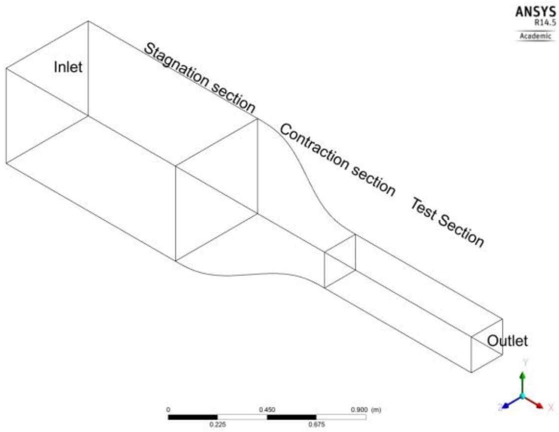

Figure 1 Real model x Numerical model

The simulations were performed in a computer with 32GB RAM, Windows 64 bits, processor Intel® Xenon® E5-1660 3.30 GHz , 1TB HD. Mesh tests were conducted, consisting of varying the maximum size of the mesh elements, with a consequent increase on the number of nodes and elements. The most refined mesh was used for analyses and dada presentation. For the mesh tests, it was set a RMS (root mean square) residual of $1.0x10^{-6}$. The average time required for the simulations with the most refined meshes was 5h18min, with an average number of nodes of 1970486.

4. EXPERIMENTAL METHODOLOGY

Experimental tests were performed in order to validate the numerical results. To a defined volume flow rate of (0,294±0,002) m³/s, corresponding to 2500 rpm from the blower, 37 points of velocity were measured. A Pitot tube was used to evaluate the velocity profile, using the recommendations from International Standard ISO 3966 (2008). The Standard recommendations are valid for Mach numbers lower than 0.25. It defines that at least 25 measurement points should be used to characterize the test section cross section, and Soares (2008) concluded that, for the wind tunnel test section, 37 points are required, shown in Fig. 2. The 37 points were evaluated both in the inlet and in the outlet of the test section.

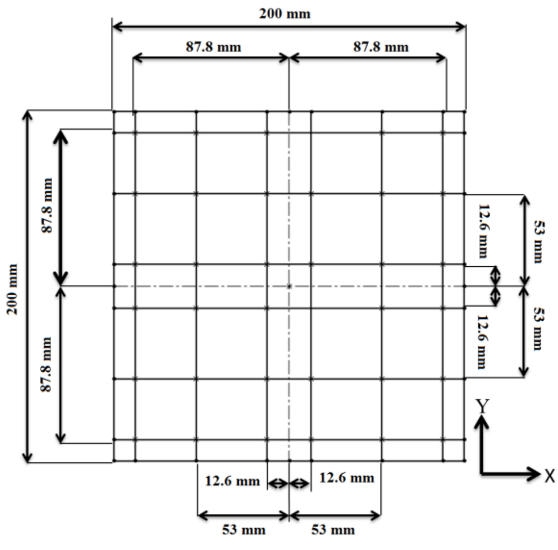

Figure 2 Positioning point distribution of Pitot tube

5. RESULTS AND DISCUSSION

According to Oberkampf e Trucano (2002), check and validation are the main methods used to evaluate the accuracy of computational simulations. It is required an experimental validation before the use of computational simulation results (Oberkamp; Trucano; Hirsch, 2004). In this paper, the validation of numerical results was made through comparison of velocity data obtained in two horizontal lines of the test section using a Pitot tube. The same y values were used in the inlet and in the outlet of the test section: 87.8 mm and 12.6 mm (Fig. 3).

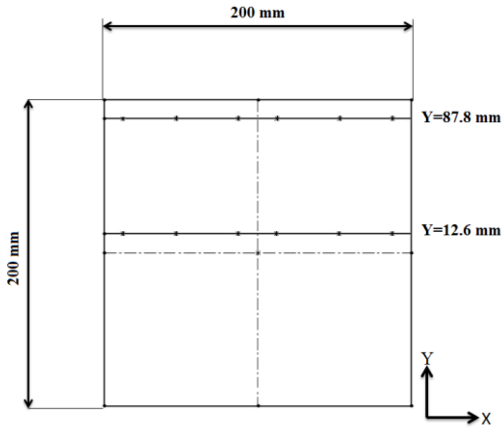

Figure 3 Validation points at line y=12.6 mm and y=87.8 mm.

Comparison between numerical and experimental data is shown in Fig. 4, for the κ-ε, κ-ω SST e BSL EARSM turbulence models. It can be seen that the numerical results are in good agreement with experimental data. Some numerical points were out of experimental uncertainty. It may be explained by the conditions imposed by the blower (with a not concentric geometry), causing a displacement of the experimental velocity profile. The EARSM model provided closer results with the Pitot tube; however, the results from SST and EARSM model are very similar.

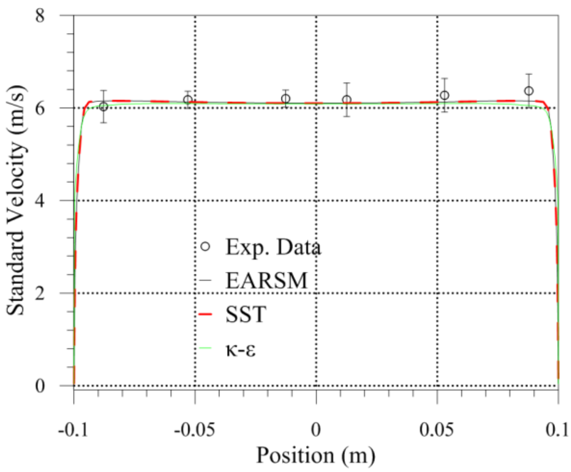

(a)

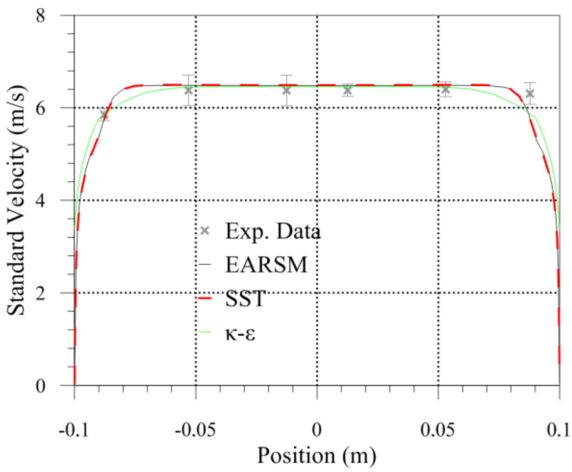

(b)

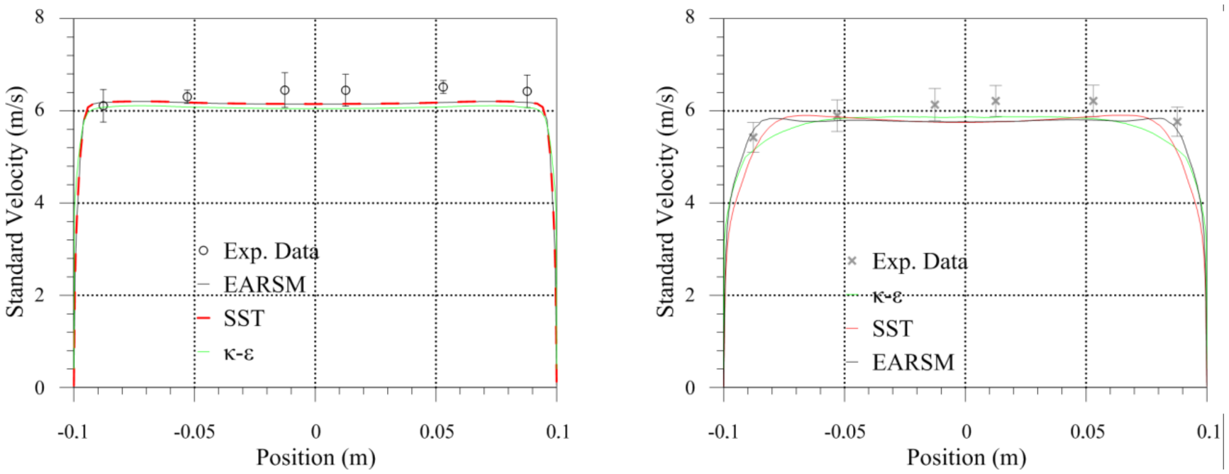

(c) (d)

Figure 4 Standard velocity per position (a) y=12.6 inlet, (b) y=12.6 mm outlet, (c) y=87.8 mm inlet, (d) y=87.8 outlet.

Figure 5 presents the turbulent kinetic energy (TKE) at the exit of the test section, obtained numerically for the three turbulence models evaluated. The results obtained were compared with the theory presented by Laufer (1953), which states that the turbulent kinetic energy is maximum close to the walls (with square edges) and minimal at the central region, where the flow can be considered free. It was examined that, despite the validation for the velocity for the three turbulence models, the κ-ε model has been unable to predict the behavior of the turbulent kinetic energy, according to the theory. It was not able to TKE in the expected way in the center of the test section. It also did not kept the expected profile close to the wind tunnel walls. According to Versteeg e Malalasekera (2007) is known that the κ-ε model is more appropriate for external flows, having poor performance for confined and rotational flows.

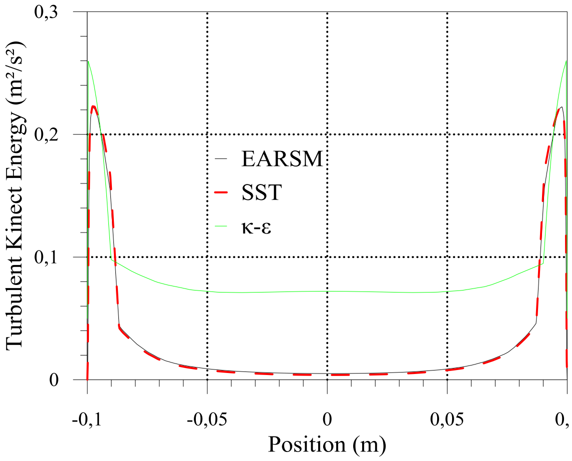

Figure 5 Turbulent Kinect Energy in the outlet of the test section

When the objects are positioned inside the test section of a wind tunnel, it is expected a uniform velocity profile, in order to simulate external conditions. For this reason, the airflow cannot be fully developed. Figure 6 presents the growth of the boundary layer along the test section, for the three turbulence models. The simulation results showed approximate values between the models, with the κ-ε presenting the thicker boundary layer in the exit of the wind tunnel. Both SST and EARSM models presented a thickness of 5.26 mm in the entrance of the test section, with SST presenting thickness of 19,83 mm at the exit and EARSM 19,60 mm. The κ-ε model predicted a value of 6,75 mm for entrance and 21,42mm for the exit. Since the EARSM and the κ-ω SST model use similar equations, the results for these models are very close to each other. Therefore, by having a lower computational cost, the model SST is more appropriate to simulate the presented problem.

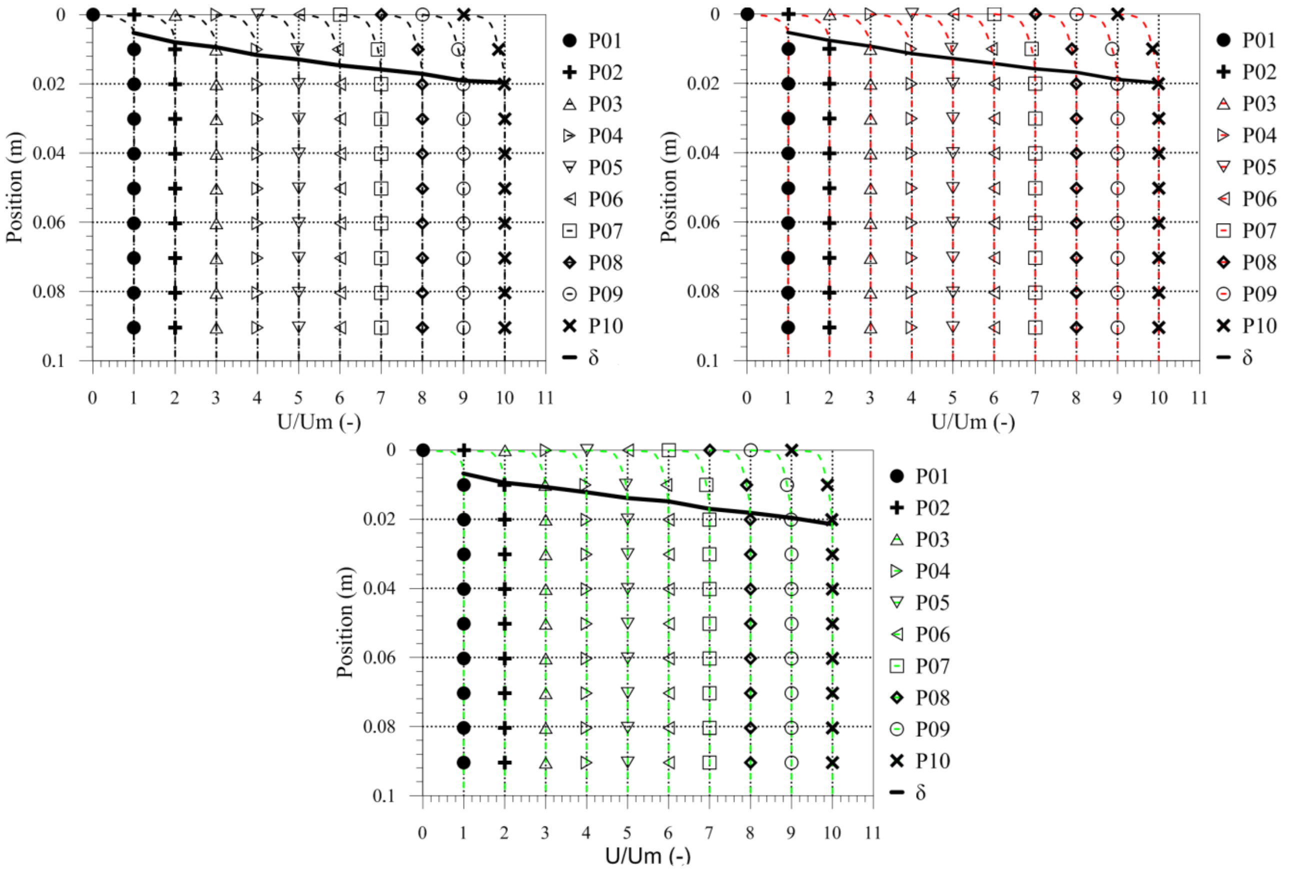

Figure 6 Boundary layer growth along the test section for (a) BSL EARSM, (b) κ-ω SST and (c) κ-ε turbulence models.

The boundary layer thickness dimensions found at the three simulations show that the flow is not fully developed, and the boundary layer thickness is much lower than the dimensions of the test section. It indicates that the wind tunnel is suitable to perform experimental tests with bodies inserted inside it.

Figure 7 presents the velocity field in the wind tunnel. The results are shown only for the κ-ω SST model. It is possible to see that the velocity is lower in the stagnation section, increasing the pressure of the airflow. Due to the reduction of the cross sectional area, the velocity increases towards the test section. It can also be seen that the velocity profile in a defined position of the test section is nearly uniform. When compared two different axial positions in the test section, it is observed that the maximum velocity increases towards the outlet, due to the increase of the boundary layer thickness.

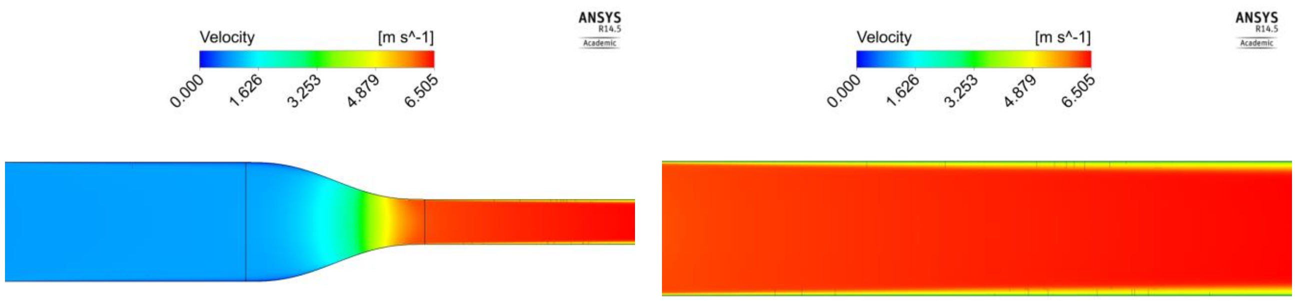

(a) (b)

Figure 7 Velocity fields (a) Wind tunnel and (b) Test section detail.

6. CONCLUSIONS

This paper evaluated the influence of three turbulence models (BSL EARSM, κ-ω SST and κ-ε) on the prediction of the airflow inside a low speed wind tunnel. Experimental tests of velocity (using a Pitot tube) were performed in order to validate numerical results, using the International Standard ISO 3966 (2008) as reference. The commercial code CFD Ansys CFX® was used to solve the governing equations of the problem.

The comparison between experimental and numerical results demonstrated that the three studied models of turbulence are capable to predict the velocities profiles at the entrance and the exit of the test section. The inconsistency of some numerical points to the three turbulence models in relation to the experimental points can be explained due to the not concentric geometry of the blower, causing a displacement of the experimental velocity profile. The κ-ε model was unable to predict the TKE profile, according to the theory presented by Laufer (1954).

The velocities and boundary layer thickness predicted by the κ-ω SST e BSL EARSM turbulence models were very similar. Since the SST model has lower computational cost, it was concluded that it is better to use the SST model to simulate the airflow inside the wind tunnel.

7. ACKNOWLEDGEMENTS

The authors are thankful to PUC Minas, FAPEMIG, CNPq and CAPES.

8. REFERENCES

Abdi, D.D., Girma,T.B., 2014. “Wind flow simulations on idealized and real complex terrain using various turbulence models”. *Advances in Engineering Software*, Vol.75, p.30-41.

Baker, C.J., 2007. “Wind engineering—Past, present and future”. *Journal of Engineering and Industrial Aerodynamics*, Vol. 95, p.843-870.

Calautit, J. K., Hughes, B. R., 2014. “Wind Tunnel and CFD study of the natural ventilation perfomance of a commercial multi-directional wind tower” *Building and Environment, Vol. 80, p 71-83.*

Calautit, J. K., Hughes, B. R., Shahzad, S. S., 2015. “CFD and wind tunnel study of the performance of a uni-directional wind catcher with heat transfer devices”. *Renewable Energy*, Vol. 83, p.85-99.

Cho, T. and Kim, C., 2011. “Wind tunnel results for a 2/4.5 scale Mexico rotor”. *Renewable Energy*, Vol.42, p.152-156.

Chung, T. J., 2002. Computational Fluid Dynamics. Cambridge University Press, Nova York, 1st edition.

Defraeye, T., Blocken, B., Koninckx, E., Hespel, P., Carmeliet, J., 2010. “Aerodynamic study off different cyclist positions: CFD analysis and full-scale wind tunnel tests”. *Journal Biomechanics*, Vol 43, p.1262-1268.

Green, J.; Quest, J.A., 2011. “Short history of the European Transonic Wind Tunnel ETW”. *Progress in AerospaceSciences*, Vol. 47, p. 319-368.

INTERNATIONAL ORGANIZATION FOR STANDARDIZATION ISO 3966, 2008. “Measurements of fluid flow in closed conduits – Velocity area method using Pitot static tubes”. Jul. 2008.

Laufer, J., 1954. “The structure of turbulence in fully developed pipe flow” National Advisory Committee for Aeronautics. 25 Jan. 2015 <http://naca.central.cranfield.ac.uk/reports/1954/naca-report-1174.pdf>.

Menter, F. R., 1992. “Influence of freestream values on κ-ω turbulence model predctions”. *American Institute of Aeronautics and Astronautics Journal*, Vol. 30, p. 1657-1659.

Merrinson, J.P. *et al*., 2008. “An environmental simulation wind tunnel for studying Aeolian transport on mars”. *Planetart and Space science*, Vol. 56, p. 426-437.

Moonen, P., Blocken, B., Roel, S., Carmeliet, J., 2006. “Numerical modeling of the flow conditions in a closed-circuit low-speed wind tunnel”. *Journal of Wind Engineering and Industrial Aerodynamics*, Vol.94, p. 699-723.

Oberkampf, W. L., Trucano, T. G., Hirsch, C., 2004. “Verification, validation, and prectivecabability in computational engineering and physics”. *Applied Mechanics and Materials*, Vol.57, p.345-384. Oberkampf, W. L., Trucano, T., 202. “Verification and validation in computacional fluid dynamics”. *Progress in Aerospace Sciences*, Vol.38, p.209-272.

Reis, M. L. C. C.; Falcão Filho, J. B. P. F.; Moraes, L. F. G., 2014. “The TTP Transonic wind tunnel Mach number uniformity analysis”. *Measurement*, Vol.51, p.-356-366.

Soares, C. B., 2008. *Estudo experimental do comportamento fluidodinâmico na seção de testes de um túnel de vento para baixas velocidades*. Master, Pontifícia Universidade Católica de Minas Gerais, Belo Horizonte.

Tong, G., Zhang, G., Christopher, D.M., Bjerg, B., Ye, Z., Cheng, J., 2012. “Evaluation of turbulence models to predict airflow and ammonia concentrations in a scale model swine building enclosure”. Computer & Fluids, Vol.71, p.240-249.

Warsi, Z. U., 2006. *A. Fluid Dynamics: Theoretical and Computational Approaches.* CRC Press, Boca Raton , 3rd edition.

9. RESPONSIBILITY NOTICE